厚生科学研究費補助金（第３次対がん総合戦略研究事業）
分担研究報告書

新戦略に基づく抗がん剤の開発に関する研究
分担研究者　上野　隆　順天堂大学医学部生化学第一講座

研究要旨：低栄養下で増殖する膵がんに対する新奇抗がん剤としてオートファジー特異的阻害剤をスクリーニングし、オートファジー特異的プロテアーゼである Atg4B に対する阻害剤の作用特性を調べた。2 種類の阻害剤 CB112B03 と CB153C07 が基底レベルのオートファジーを強く阻害することを見出した。

A.　研究目的

低栄養・低酸素条件下で盛んに増殖する膵がんは、細胞自身のタンパクをターンオーバーする機構であるオートファジーを利用してその産物であるアミノ酸や脂肪酸を代謝してエネルギーを獲得している可能性が指摘されてきた。分担者はこれまで培養膵がん細胞 PANC-1 を材料として Kigamicin D がアミノ酸欠乏ではなくグルコース欠乏にのみ応答してそのタンパク分解を有意に阻害することを明らかにしてきた。ところで、膵がんがオートファジーを生存戦略として利用しているという仮説に立てば、新たなオートファジー阻害剤を開発して膵がんに対する作用を明らかにする展望が求められる。そこで、百瀬功と共同でこの阻害剤開発・スクリーニングに取り組むこととした。オートファジーには 20 種類以上の遺伝子（ATG 遺伝子）の働きが必須であるが、中でも Atg4B はシステインプロテアーゼの活性を持ち、オートファゴソーム膜マーカーである LC3 のプロセシングに必須である。そこで Atg4B を特異的に阻害する薬剤はオートファジーを効率よく阻害することが期待される。Atg4B の立体構造は結晶解析から既に明らかにされているので、百瀬はまず TR-FRET 法による鋭敏な Atg4B 活性測定法を確立し、in vitro アッセイによって、特異的に阻害作用を持つ化合物をスクリーニングした。

B. 研究方法

１）長寿命タンパク分解測定

百瀬によってスクリーニングされた阻害剤を培養肝細胞に加え、長寿命タンパク分解に対する効果を測定し、オートファジーを阻害するかを調べた。すなわち、14C-ロイシンで初代培養肝細胞を 22 時間標識、さらに 2 時間のチェイスを経て、栄養欠乏条件下（STV）と富栄養条件下（NSTV）でのタンパク分解を測定する。

２）ウェスタンブロットによる LC3-II の検出とオートファジーフラックス測定

１）と関連して、NSTV および STV での肝細胞や HeLa 細胞の LC3-II レベルを調べる。LC3-II はオートファジーが誘導されてオートファゴソーム

が形成されるにしたがって増加するが、オートファゴソームがオートリソソームに熟成するとリソソームで分解されてむしろ減少する。その際E64dやpepstatinを加えておくとオートリソソームでの LC3-II の分解が抑えられて LC3-II は顕著に増加する。E64d/ pepstatin 存在下非存在下のLC3-IIのシグナル差(LC3-IIフラックス）がおおまかにオートファジーの活性を表すことが知られているので、スクリーニングされたAtg4B 阻害剤が結果的にオートファジーを阻害することによって LC3-II フラックスを阻害するかを確かめた。

（倫理面への配慮）マウス肝細胞単離に際しては、「倫理的基準に基づいたヒト以外の動物種を用いた医学生物学実験の分類」のカテゴリーBに従った。

C. 研究結果

1）Atg4B 阻害剤の長寿命タンパク分解への効果

マウス初代培養肝細胞の長寿命タンパクに対して、Atg4B 阻害剤は興味深い作用を及ぼした。7 種類の阻害剤 (CB06D04、CB08C07、CB23A11、CB25D05 、 CB27D04 、 CB112B03 、CB153C07)のうち、CB06D04、CB08C07、CB23A11、CB25D05、CB27D04 については長寿命タンパク分解への影響はほとんど見られなかったが、CB112B03 と CB153C07 はNSTV でのタンパク分解を強く阻害する一方、STVでの分解にはほとんど影響が無かった。

2）オートファジーフラックスへのAtg4B 阻害剤の効果

1）の結果と関連して、オートファジーフラックスをウェスタンブロットで調べた。その結果、長寿命タンパク分解への効果と同様、CB112B03 と CB153C07 はNSTV でのオートファジーフラックスを強く阻害したが、他の阻害剤は目立った阻害効果を現さなかった。

D. 考察

百瀬が確立した TR-FRET 法では、Atg4B の基質である LC3 の C 末端に myc タグ、N 末に FLAG タグを連結させて、それぞれのタグを認識する抗体に蛍光プローブが結合している。2つの蛍光分子のエネルギー遷移は、Atg4B によって LC3 の C 末 myc タグとの間が切断されることによって解消される。この測定法により感度の高い Atg4B 活性が測定できるようになった。

スクリーニングされた 7 種類の阻害剤のうち CB112B03 と CB153C07 のみが長寿命タンパク分解や LC3-II のオートファジーフラックスを強く阻害した。他の阻害剤が細胞に効果を及ぼさない点については、これらの阻害剤が細胞膜を透過しにくく細胞質へ浸透しない可能性が有る。これは今後確認を要する。一方、CB112B03 と CB153C07 の効果についても解らないことがある。なぜ基底レベル (NSTV) でのオートファジーにしか影響を及ぼさないのかというのは不可解である。Atg4B のシステインプロテアーゼとしての働きについては解らないことも多いので、今後 Atg4B の作用特性を明らかにする意味でも更なる解析が非常に重要となる。

E. 結論

CB112B03 と CB153C07 は Atg4B 阻

害作用と関連した強い基底レベルオートファジー阻害活性を有するユニークな阻害剤で、膵がん細胞への効果を含めてさらに検討していきたい。

対がん総合戦略事業の一環として研究を行う立場から抗がん剤 Adriamycin による腎症の機構を調べた。糸球体微少環境維持に重要な貢献を行っている足場細胞へのアドリアマイシンの阻害効果において、dendrin が足場細胞表層から核へ移行することを明らかにした。その結果を論文として発表した。

F. 健康危険情報

特になし。

G. 研究発表

論文発表

Katsuhiko Asanum, Miyuki Akiba-Takagi, Fumiko Kodama et al. Dendrin location in podocytes is associated with the disease progression in animal and human glomerulopathy. Am. J. Nephrol. in press

H. 知的財産権の出願・登録状況

1. 特許取得

なし

2. 実用新案登録

なし

3. その他

なし

厚生科学研究費補助金（第３次対がん総合戦略研究事業）
分担研究報告書

新戦略に基づく抗がん剤の開発に関する研究

分担研究者　丸山　一雄　帝京大学　教授

研究要旨：がん遺伝子治療は、新たながん治療戦略の１つとして期待されている。しかし、安全性が高いとされている非ウイルスベクターの開発が遅れており、安全で有効ながん遺伝子治療の確立には至っていない。これまでに我々は、超音波照射によるリポソーム型ナノバブル（バブルリポソーム）のキャビテーションを利用した新規遺伝子導入法を開発した。そこで本研究では、バブルリポソームと超音波照射の併用によるがん遺伝子治療への応用に関する検討を行った。強力な抗腫瘍効果を有するサイトカインであるインターロイキン-12 を発現する遺伝子を本方法によりがん組織に遺伝子導入したところ、がん治療効果が認められた。このことから、本遺伝子導入法が有効ながん遺伝子治療を構築する上で有望な非ウイルスベクターとして利用可能になることが示唆された。

A. 研究目的

インターロイキン-12（IL-12）は、強力な抗腫瘍効果を誘導できるサイトカインである。しかし、IL-12 の全身投与は、全身性副作用の発現が懸念されている。副作用の影響なく治療効果を得るためには、がん組織で局所的に IL-12 を作用させる必要がある。そのため、がん組織で IL-12 を発現させる IL-12 遺伝子治療が注目されている。しかし、遺伝子送達に関して安全で有効な非ウイルスベクターは確立されていない。これまでに我々は、既存の非ウイルスベクターとして汎用されているカチオニックリポソームを用いたリポフェクション法より効率よく in vivo 組織に対して遺伝子導入可能な超音波遺伝子導入法を開発した。この方法では、リポソームに超音波造影ガスを封入したリポソーム型ナノバブル（バブルリポソーム）に超音波照射した時に生じるジェット流を駆動力に細胞内に効率よく遺伝子を導入可能である。そこで本研究では、IL-12 がん遺伝子治療におけるバブルリポソームと超音波照射の併用による遺伝子導入伝子導入法の有用性を評価した。

B. 研究方法

<u>バブルリポソームと超音波照射の併用によるがん組織への遺伝子導入効率の評価</u>

マウス卵巣がん細胞（OV-HM 細胞）を B6C3F1 マウスの後背部皮内に移植した。その７日後、バブルリポソーム（2.5 μg）と IL-12 発現プラスミド DNA

(pCMV-IL12: 10 μg) を固形がん組織内に投与し、速やかに体外から超音波照射した。その後、IL-12 の発現を評価するため、がん組織における IL-12p40 mRNA の発現を RT-PCR にて検討した。なお、比較検討として pCMV-IL12 (10 μg) と Lipofectamine 2000 (LF2000) (20 μg) のリポプレックスを腫瘍内投与した群についても同様の検討を行った。

バブルリポソームと超音波照射の併用による IL-12 遺伝子導入におけるがん遺伝子治療効果の検討

マウス卵巣がん細胞 (OV-HM 細胞) を B6C3F1 マウスの後背部皮内に移植し 7 日後に 1 回または 7、9、12、14、16、19 日の計 6 回、バブルリポソーム (2.5 μg) と IL-12 発現プラスミド DNA (pCMV-IL12: 10 μg) を腫瘍内に投与し、速やかに体外から超音波照射した。その後の腫瘍体積を指標にがん治療効果を検討した。なお、比較検討として pCMV-IL12 (10 μg) と LF 2000 (20 μg) のリポプレックスを腫瘍内投与した群についても同様の検討を行った。

C. 研究結果

バブルリポソームと超音波照射の併用によるがん組織への遺伝子導入効率の評価

pCMV-IL12 単独投与群、pCMV-IL12 とバブルリポソーム投与群、pCMV-IL12 単独投与後に超音波照射した群では、ほとんど IL-12p40 mRNA の発現は認められなかった。LF2000 による pCMV-IL12 遺伝子導入群では、遺伝子導入 1 日後に若干の IL-12p40 の発現が認められたが、2 日後にその発現は消失した。一方、バブルリポソームと超音波照射の併用群では、2 日後でも IL-12p40 mRNA の発現が認められた (図 1)。このことから、バブルリポソームと超音波照射の併用により効率よくがん組織に IL-12 が発現しているものと推察された。

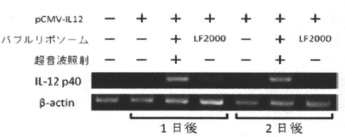

図1 バブルリポソームと超音波照射の併用によるがん組織への IL-12 発現遺伝子導入効率

バブルリポソームと超音波照射の併用による IL-12 遺伝子導入におけるがん遺伝子治療効果の検討

pCMV-IL12 単独投与群、pCMV-IL12 とバブルリポソーム投与群、pCMV-IL12 単独投与後に超音波照射した群や LF2000 による pCMV-IL12 遺伝子導入群では、ほとんど腫瘍増殖抑制効果は認められなかった。一方、pCMV-IL12 とバブルリポソームを投与後に超音波照射した群では、顕著な腫瘍増殖抑制効果が認められた (図 1 (a))。これは、前項で検討した IL-12 の発現量に起因しているものと考えられ

た。しかし、本検討においてバブルリポソームと超音波照射の併用群においても

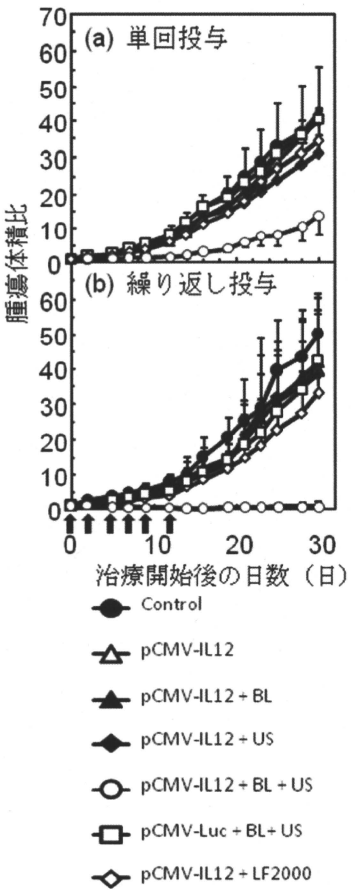

図2　バブルリポソームと超音波照射の併用によるIL-12がん遺伝子治療効果

完全治癒例は認められなかった。これは、本遺伝子導入法による遺伝子発現が一過性であるためと考えられた。そこで、がん組織での IL-12 発現維持を目的に繰り返し遺伝子導入を行った際のがん治療効果を検討した（図２（ｂ））。その結果、pCMV-IL12 とバブルリポソームを投与後に超音波照射した群においてのみ、80 %のマウスで完全治癒が認められた。このことから、バブルリポソームと超音波照射の併用による遺伝子導入を繰り返すことで、IL-12 のがん組織における有効濃度が維持されて強力な腫瘍免疫が誘導されたものと考えられた。

E. 結論

バブルリポソームと超音波の併用による遺伝子導入法は IL-12 がん遺伝子治療において有用な非ウイルスベクターになることが示唆された。このことから、本遺伝子導入法ががん遺伝子治療に対する安全で有効なウイルスを使用しない遺伝子導入システムとして幅広く利用可能になるものと期待される。

F. 健康危険情報

該当無し

G. 研究発表

1. 論文発表

1) Progress in the development of ultrasound-mediated gene delivery

systems utilizing nano- and microbubbles. Suzuki R, Oda Y, Utoguchi N, Maruyama K, J. Control. Release. 149(1), 36-41, 2011

2) Circadian Rhythm of Transferrin Receptor 1 Gene Expression Controlled by c-Myc in Colon Cancer-Bearing Mice. Okazaki F, Matsunaga N, Okazaki H, Utoguchi N, Suzuki R, Maruyama K, Koyanagi S, Ohdo S. Cancer Res. 70 (15), 6238-6246, 2010

3) Development of an ultrasound -responsive and mannose-modified gene carrier for DNA vaccine therapy. Un K, Kawakami S, Suzuki R, Maruyama K, Yamashita F, Hashida M, Biomaterials. 31(30), 7813-26, 2010

4) Effective in vitro and in vivo gene delivery by the combination of liposomal bubbles (bubble liposomes) and ultrasound exposure. Suzuki R, Maruyama K, Methods Mol. Biol. 605, 473-86, 2010

5) Synergistic effect of ultrasound and antibiotics against Chlamydia trachomatis-infected human epithelial cells in vitro. Ikeda-Dantsuji Y, Feril LB Jr, Tachibana K, Ogawa K, Endo H, Harada Y, Suzuki R, Maruyama K, Ultrason. Sonochem. 18(1), 425-30, 2010

6) Cancer gene therapy by IL-12 gene delivery using liposomal bubbles and tumoral ultrasound exposure. Suzuki R, Namai E, Oda Y, Nishiie N, Otake S, Koshima R, Hirata K, Taira Y, Utoguchi N, Negishi Y, Nakagawa S, Maruyama K, J. control. Release, 142, 245-50, 2010

7) Optimum conditions of ultrasound -mediated destruction of bubble liposome for siRNA transfer in bladder cancer. Fujisawa S, Arakawa H, Suzuki R, Maruyama K, Kodama T, Yasunaga M, Koga Y, Matsumura Y. Therapeutic Delivery, 1(2), 247-255, 2010

2. 学会発表

1. 鈴木　亮、**丸山一雄**「リポソーム製剤」リポソーム技術を基盤とした新たなＤＤＳ戦略、ナノメディシン研究会、東京、平成22年9月
2. 鈴木　亮、**丸山一雄**、リポソーム技術と超音波技術を基盤とした革新的がん治療システムの構築、ソノプロセス分科会シンポジウム、東京、平成23年10月
3. Suzuki R, **Maruyama K**、Cancer immunotherapy utilized ultrasound

sensitive liposomes (Bubble liposomes)、the 2010 FIP PSWC/AAPS Annual Meeting and Exposition、ニューオリンズ（米国）、平成22年11月

H. 知的財産権の出願・登録状況

1. 特許取得

該当無し

2. 実用新案登録

該当無し

3. その他

該当無し

別紙４

研究成果の刊行に関する一覧表

雑誌

発表者氏名	論文タイトル名	発表誌名	巻号	ページ	出版年
J Kuroda, Y Matsumura, et al.	Antitumor Effect of NK012, SN-38 Incorporating Polymeric Micelle on U87MG OrthotopicGlioblastoma in Mice Compared with Irinotecan in Combination with Bevacizumab.	Clin Cancer Res	15;16(2)	521-9	2010
H Kenmotsu, Y Matsumura, et al.	The antitumor activity of NK012, a SN-38 incorporating micelle, in combination with bevacizumab against lung cancer xenografts.	Cancer	October 1	4597-4604	2010
T Nagano, Y Matsumura, et al.	Synergistic Antitumor Activity of the SN-38-Incorporating Polymeric Micelles NK012 with S-1 in a Mouse Model of Non-Small Cell Lung Cancer.	Int J Cancer	127(11)	2699-2706	2010
A Takahashi, Y Matsumura, et al.	Detailed distribution of NK012, an SN-38 incorporating micelle, in the liver and its potent antitumor effects in mice bearing liver metastases.	Clin Cancer res	16(19)	4822-4831	2010
S Fujisawa, Y Matsumura, et al.	Optimum conditions of ultrasound-mediated destruction of bubble liposome for siRNA transfer in bladder cancer.	Therapeutic Delivery	1(2)	247-255	2010
Y Matsumura, et al.	Preclinical and clinical studies of NK012, an SN-38-incorporating polymeric micelles, which is designed based on EPR effect.	Adv Drug Deliv Rev	63(3)	184-192,	2010
T Hamaguchi, Y Matsumura, et al.	Phase I Study of NK012, a Novel SN-38–Incorporating Micellar Nanoparticle, in Adult Patients with Solid Tumors.	Clin Cancer Res	16(20)	5058-5066	2010

発表者氏名	論文タイトル名	発表誌名	巻号	ページ	出版年
A Ishii-Watabe, Y Matsumura, et al.	Genetic polymorphisms of FCGRT encoding FcRn in a Japanese population and their functional analysis.	Drug Metab Pharmacokinet			2010
R Plummer, Y Matsumura, T Nishiya, et al.	A phase I clinical study of cisplatin-incorporated polymeric micelles (NC-6004) in patients with solid tumors.	Brit J Cancer	15;104(4)	593-8	2011
Yasunaga M, Y Matsumura, et al.	New Concept of Cytotoxic Immunoconjugate Therapy Targeting Cancer-Induced Fibrin Clots.	Cancer Sci	in press		2011
I Momose, et al.	Mitochondrial inhibitors show preferential cytotoxicity to human pancreatic cancer PANC-1 cells under glucose-deprived conditions.	Biochem Biophys Res Commun	392	460-466	2010
M Kawada, I Momose, et al.	Leucinostatin A inhibits prostate cancer growth through reduction of insulin-like growth factor-I expression in prostate stromal cells.	Int J Cancer	126	810-818	2010
M Iijima, I Momose, et al.	Increased ABCB1 expression in TP-110-resistant RPMI-8226 cells.	Biosci Biotechnol Biochem	74	1913-1919	2010
T Watanabe, I Momose, et al.	Structure-activity relationship of boronic acid derivatives of tyropeptin: proteasome inhibitors.	Bioorg Med Chem Lett	20	5839-5842	2010

発表者氏名	論文タイトル名	発表誌名	巻号	ページ	出版年
K Asanuma, T Ueno, et al.	Dendrin location in podocytesis associated with the diseaseprogression in animal and human glomerulopathy.	Am. J. Nephrology	In press		2011
M. Murakami, N. Nishiyama, et al.	Improving drug potency and efficacy by nanocarrier-mediated subcellular targeting.	Science Transl. Med	3(64)	64ra2	2011
S. Kaida, N. Nishiyama, et al.	Visible-drug delivery by supramolecular nanocarriers directing to single-platformed diagnosis and therapy of pancreatic tumor model.	Cancer Res	70(18)	7031-7041	2010
Onozuka H, Tsuchihara K, Esumi H, et al	Hypoglycemic/hypoxic condition in vitro mimicking the tumor microenvironment markedly reduced the efficacy of anticancer drugs.	Cancer Sci	102(5)	975-982	2011
Suzuki R, Maruyama K, et al.	Progress in the development of ultrasound-mediated gene delivery systems utilizing nano- and microbubbles.	J. Control. Release	149	36-41	2011
Okazaki F, Maruyama K, Ohdo S, et al.	Circadian Rhythm of Transferrin Receptor 1 Gene Expression Controlled by c-Myc in Colon Cancer-Bearing Mice.	Cancer Res.	70	6238-6246	2010
Un K, Maruyama K, Hashida M, et al.	Development of an ultrasound-responsive and mannose-modified gene carrier for DNA vaccine therapy.	Biomaterials	31	7813-26	2010
Suzuki R, Maruyama K, et al.	Effective in vitro and in vivo gene delivery by the combination of liposomal bubbles (bubble liposomes) and ultrasound exposure.	Methods Mol. Biol	605	473-86	2010

発表者氏名	論文タイトル名	発表誌名	巻号	ページ	出版年
Ikeda-Dantsuji Y, Maruyama K, et al.	Synergistic effect of ultrasound and antibiotics against Chlamydia trachomatis-infected human epithelial cells in vitro.	Ultrason. Sonochem	18	425-30	2010
Suzuki R, Maruyama K, et al.	Cancer gene therapy by IL-12 gene delivery using liposomal bubbles and tumoral ultrasound exposure.	J. control. Release	142	245-50	2010

Cancer Therapy: Preclinical

Clinical Cancer Research

Antitumor Effect of NK012, a 7-Ethyl-10-Hydroxycamptothecin–Incorporating Polymeric Micelle, on U87MG Orthotopic Glioblastoma in Mice Compared with Irinotecan Hydrochloride in Combination with Bevacizumab

Jun-ichiro Kuroda[1,2], Jun-ichi Kuratsu[2], Masahiro Yasunaga[1], Yoshikatsu Koga[1], Hirotsugu Kenmotsu[1], Takashi Sugino[3], and Yasuhiro Matsumura[1]

Abstract

Purpose: To clarify the effect of bevacizumab on NK012 therapy in mice bearing U87MG glioblastoma orthotopic xenografts in comparison with the combination therapy of irinotecan hydrochloride (CPT-11) with bevacizumab.

Experimental Design: NK012 at 7-ethyl-10-hydroxycamptothecin (SN-38) equivalent dose of 30 mg/kg was administered intravenously three times every 4 days with or without bevacizumab. CPT-11 at 66.7 mg/kg was administered intravenously three times every 4 days or CPT-11 at 40 mg/kg/d over 5 consecutive days with or without bevacizumab. Bevacizumab was administered intraperitoneally six times every 4 days in each experiment. *In vivo* antitumor effects were evaluated by bioluminescence imaging, histopathologic evaluation, and immunohistochemistry. To evaluate interaction with bevacizumab, free SN-38 concentration in tumor tissues was examined by high-performance liquid chromatography.

Results: CPT-11 in combination with bevacizumab showed significantly more potent antitumor activity and longer survival than CPT-11 monotherapy ($P < 0.05$). However, there was no difference between NK012 monotherapy and NK012 in combination with bevacizumab. Concentration of free SN-38 released from NK012 in tumor tissue decreased in combination with bevacizumab ($P = 0.027$). NK012 monotherapy or NK012 with bevacizumab showed potent antitumor activity and longer survival than any dosing method of CPT-11 in combination with bevacizumab ($P < 0.05$). Orthotopic tumors treated with NK012 showed decreased tumor cellularity and lower Ki-67 index ($P < 0.001$) relative to those treated with CPT-11/bevacizumab.

Conclusions: The present study using orthotopic glioblastoma model in mice may warrant further preclinical evaluation of NK012 before conducting the clinical trial of the drug, because the antitumor activity of NK012 monotherapy was superior to the combination therapy of CPT-11 with bevacizumab.
Clin Cancer Res; 16(2); 521–9.

Malignant glioma, such as glioblastoma multiforme and anaplastic astrocytoma, are the most commonly occurring primary malignant brain tumors, and glioblastoma multiforme is well known as a typical hypervascular tumor with a high expression level of vascular endothelial growth factor (VEGF; ref. 1). Currently, glioblastoma multiforme patients have a mean survival time of only 50 weeks following the standard treatment consisting of surgical and adjuvant therapies (2). However, a recent phase III randomized trial for newly diagnosed glioblastoma multiforme showed that radiation therapy with concurrent temozolomide treatment followed by 6 months of temozolomide treatment was superior to radiation therapy alone in terms of overall survival (3). Furthermore, several clinical trials have shown that the median survival time of patients with recurrence was only 30 weeks (4). Therefore, a novel antitumor agent based on a new approach for the recurrent malignant glioma is eagerly awaited.

7-Ethyl-10-hydroxycamptothecin (SN-38) is a broad-spectrum anticancer agent targeting DNA topoisomerase I. Irinotecan hydrochloride (CPT-11), a prodrug of SN-38, shows some antitumor activity in patients with recurrent glioblastoma multiforme, with response rates of 0 to 17% in several trials (5–8). CPT-11 single-agent chemotherapy activity is thus similar to that of other agents used for

Authors' Affiliations: [1]Investigative Treatment Division, Research Center for Innovative Oncology, National Cancer Center Hospital East, Kashiwa, Japan; [2]Department of Neurosurgery, Faculty of Medical and Pharmaceutical Sciences, Kumamoto University, Kumamoto, Japan; and [3]Department of Pathology, Fukushima Medical University School of Medicine, Fukushima, Japan

Corresponding Author: Yasuhiro Matsumura, Investigative Treatment Division, Research Center for Innovative Oncology, National Cancer Center Hospital East, 6-5-1 Kashiwanoha, Kashiwa 277-8577, Japan. Phone: 81-4-7134-6857; Fax: 81-4-7134-6857; E-mail: yhmatsum@east.ncc.go.jp.

doi: 10.1158/1078-0432.CCR-09-2393

Translational Relevance

A recent phase II trial for recurrent glioblastoma multiforme showed that irinotecan hydrochloride (CPT-11) combined with bevacizumab is a promising and unprecedentedly effective treatment against the recurrent glioblastoma multiforme. However, there may be an increasing risk of developing venous thrombotic disease and intracranial hemorrhage with this combination therapy. The 7-ethyl-10-hydroxycamptothecin–incorporating polymeric micelle NK012 has been shown to have significant antitumor activity against several cancer mouse models compared with CPT-11. Two phase I trials in Japan and the United States showed that patients treated with NK012 did not develop grade 3/4 diarrhea, one of the major adverse effects of CPT-11. Here, NK012 showed potent antitumor activity and longer survival than CPT-11 in combination with bevacizumab in glioblastoma multiforme orthotopic tumor in mice. These results warrant clinical evaluation in patients with malignant glioma.

recurrent glioblastoma multiforme (7). Meanwhile, glioblastoma cells express high levels of VEGF *in situ*. Accordingly, antiangiogenic strategies may be a promising approach for malignant gliomas hypervascular in nature. A recent phase II trial for recurrent glioblastoma multiforme showed that CPT-11 combined with bevacizumab, an anti-VEGF monoclonal IgG1 antibody, is a promising and unprecedentedly effective treatment against the recurrent malignant glioma with a 6-month progression-free survival rate of 46% and a 6-month overall survival rate of 77% (9, 10). On the other hand, there may be an increased risk of developing venous thromboembolic disease and intracranial hemorrhage with this combination therapy. Therefore, it is reasonable to develop other available treatment modalities by which cytotoxic drugs can exert more potent antitumor activity to their full potential with modest adverse effects and thereby reasonably prolong the overall survival of recurrent glioblastoma multiforme patients.

NK012, a SN-38–incorporating polymeric micelle, is a prodrug of SN-38 similar to CPT-11. Polymer-conjugated drugs categorized under drug delivery system agents are favorably extravasated from tumor vessels into the interstitium of tumors due to the enhanced permeability and retention effect (11, 12). The enhanced permeability and retention effect is based on the following pathophysiologic characteristics of solid tumor tissues: hypervascularity; incomplete vascular architecture; secretion of vascular permeability factors stimulating extravasation within cancer tissue; and absence of effective lymphatic drainage from the tumors, which impedes the efficient clearance of macromolecules accumulated in solid tumor tissues. Moreover, macromolecules cannot freely leak out from normal vessels; thus, the adverse effect of an anticancer agent can be reduced. Very recently, we showed that NK012 exerted significantly more potent antitumor activity against several kinds of tumors including human glioma in xenograft models (13). In the present study, we report the antitumor activity of NK012 compared with CPT-11 combined with bevacizumab against orthotopic U87MG glioblastoma in nude mice.

Materials and Methods

Drugs. NK012 was supplied by Nippon Kayaku. Lyophilized NK012 was dissolved in sterile distilled water at a concentration of 5 mg/mL (SN-38 equivalent dose) just before administration to mice. The size of NK012 was ~20 nm in diameter with a narrow size distribution (12). CPT-11 was purchased from Yakult Honsha. Bevacizumab was purchased from Chugai Pharmaceutical.

Cell cultures. The human glioblastoma cell line U87MG was obtained directly from the American Type Culture Collection. A U87MG cell line clone stably expressing firefly luciferase named U87MG/Luc was established from polyclonal U87MG/Luc reported previously (13). The sensitivity of U87MG/Luc cells to NK012 and CPT-11 was almost similar to that of parental U87MG cells (data not shown). U87MG/Luc cells were maintained in DMEM supplemented with 10% fetal bovine serum (Cell Culture Technologies), penicillin, streptomycin, and amphotericin B (100 units/mL, 100 μg/mL, and 25 μg/mL, respectively; Sigma) in a humidified atmosphere containing 5% CO_2 at 37°C.

In vivo *orthotopic model and imaging.* Six- to 8-week-old female athymic BALB/c *nu/nu* mice (Charles River Japan) were used for this study. U87MG/Luc cells (5×10^5) suspended in 5 μL PBS were injected into the right frontal lobe of each mouse as described previously (13). *In vivo* bioluminescence imaging studies were done using the Photon Imager animal imaging system (BioSpace). For imaging, mice with intracranial U87MG/Luc tumor were simultaneously anesthetized with isoflurane, and D-luciferin potassium salt (Synchem) was intraperitoneally administered at a dose of 2.5 mg/mouse. For bioluminescence image analysis, regions of interest encompassing the intracranial area of a signal were defined using Photo Vision software (BioSpace), and the total number of photons per minute [counts/min (cpm)] was recorded. The pseudo-color luminescent image represented the spatial distribution of detected photon counts emerging from active luciferase within the animal. All animal procedures were done in compliance with the Guidelines for the Care and Use of Experimental Animals established by the Committee for Animal Experimentation of the National Cancer Center, Japan; these guidelines meet the ethical standards required by law and also comply with the guidelines for the use of experimental animals in Japan.

In vivo *tumor growth inhibition assay.* Eight days after inoculation of U87MG/Luc cells into the right hemisphere of the brain, mice with cpm >2,000 were randomly assigned into eight test groups of five mice

(2,296-15,624 cpm). After the randomization of mice based on cpm, we confirmed that the mean value of cpm was statistically identical between groups.

Treatment was started (day 0; Table 1). *In vivo* bioluminescence imaging was done by Photon Imager and luciferase activity was measured once a week (days 0, 7, 14, 21, 28, and 35). Body weight of each mouse of the treatment experiment was also measured once a week (days 0, 7, 14, 21, 28, and 35), and mortality and morbidity were checked daily from the day of treatment initiation. Simultaneously, to assess the survival of mice with intracranial U87MG/Luc tumor, mice were maintained until each animal showed signs of morbidity (20% weight loss and neurologic deficit), at which point they were sacrificed.

In all groups, the total dose of NK012 and CPT-11 was 90 mg/kg (SN-38 equivalent dose) and 200 mg/kg, respectively. A total dose of 200 mg/kg was shown previously to be the maximum tolerated dose (MTD) of CPT-11 in nude mice (14, 15). As CPT-11 is a schedule-dependent anticancer agent, it was administered under two different treatment regimens (16). Each drug was administered according to the mouse body weight: (*a*) normal 0.9% NaCl solution (q4d × 4, intravenously), (*b*) NK012 (30 mg/kg, q4d × 3, intravenously), (*c*) CPT-11 (66.7 mg/kg, q4d × 3, intravenously), (*d*) CPT-11 (40 mg/kg, qd × 5, intravenously), (*e*) bevacizumab (5 mg/kg, q4d × 6, intraperitoneally), (*f*) NK012 (30 mg/kg, q4d × 3, intravenously) with bevacizumab (5 mg/kg, q4d × 6, intraperitoneally), (*g*) CPT-11 (66.7 mg/kg, q4d × 3, intravenously) with bevacizumab (5 mg/kg, q4d × 6, intraperitoneally), or (*h*) CPT-11 (40 mg/kg, qd × 5, intravenously) with bevacizumab (5 mg/kg, q4d × 6, intraperitoneally) was administered to the mice (Table 1). In the case of combination therapy, drugs were administered concomitantly.

Evaluation of antitumor activity. The antitumor activity of each treatment was evaluated according to three criteria: (*a*) number of tumor regressions, (*b*) tumor growth delay, and (*c*) Kaplan-Meier analysis to determine the effect on the time to morbidity. Decrease >50% of the initial photon count (cpm) was defined as a tumor regression. It had to be observed for at least two consecutive photon-counting events to be retained. Tumor growth delay was defined as the difference in the median time to reach a photon count of 5-fold compared with that of day 0 between the treated group and the control group (14). To evaluate the change in photon count of each treatment group, repeated-measures ANOVA was carried out using the StatView 5.0 software package. $P < 0.05$ was regarded as significant. Statistical differences in the Kaplan-Meier curve of each group were ranked according to the Breslow-Gehan-Wilcoxon test using StatView 5.0.

Immunohistochemistry. Histologic sections were taken from U87MG/Luc orthotopic tumor tissues at day 15 from the initiation of each therapy. The time points for analysis were chosen according to when the best antitumor activity was obtained. The brain was removed from the skull, fixed in buffered 4% paraformaldehyde, embedded in paraffin, and then cut into 3-μm-thick sections. Conventional H&E-stained sections were prepared for general histopathologic evaluation. Immunohistochemistry was done using antibodies to human Ki-67 (BD Pharmingen), human VEGF (Santa Cruz Biotechnology), and mouse CD34 (MEC 14.7; Abcam). For antigen retrieval, sections were autoclaved in Dako REAL Target Retrieval Solution (Dako Denmark). Detection was done by Vectastain Elite avidin-biotin complex kit (Vector Laboratories) for CD34 and EnVision$^+$ system labeled polymer-horseradish peroxidase anti-mouse (DakoCytomation) for Ki-67 and anti-rabbit for VEGF. The proliferation index was evaluated by counting Ki-67$^+$ cells per 1,000 tumor cells using ImagePro Plus analysis software. VEGF immunoreactivity area was quantified using the analysis software BZ Analyzer (Keyence) with a constant color threshold in 10 high-power fields per slide (×400) and is given in percent of positive area in field of view. Tumor vascularity was assessed by counting CD34$^+$ microvessels in 10 high-power fields per slide (×400). The small intestine was sampled at 5 cm from the pylolic part for the jejunum and 5 cm

Table 1. Activity of three anticancer drugs against orthotopic U87MG xenografts

Treatment course	Dose (mg/kg/d)	Schedule	Total dose (mg/kg)	No. animals/ group	Maximum body weight loss (%)	Toxic death	Tumor regression	Tumor growth delay (d)	Median overall survival (d)
Control	—	—	—	5	—	—	—	—	29
NK012	30	q4d × 3	90	5	3.8	0	3	>18	48
CPT-11	66.7	q4d × 3	200	5	6.6	0	0	8	36
CPT-11	40	qd × 5	200	5	2	0	1	8	34
Bevacizumab	5	q4d × 6	30	5	1.9	0	0	4	40
NK012/bevacizumab	30/5	q4d × 3/q4d × 6	90/30	5	0.9	0	1	12	46
CPT-11/bevacizumab	66.7/5	q4d × 3/q4d × 6	200/30	5	0	0	2	7	40
CPT-11/bevacizumab	40/5	qd × 5/q4d × 6	200/30	5	0.7	0	2	8	41

NOTE: Maximum body weight loss (days 0-28).

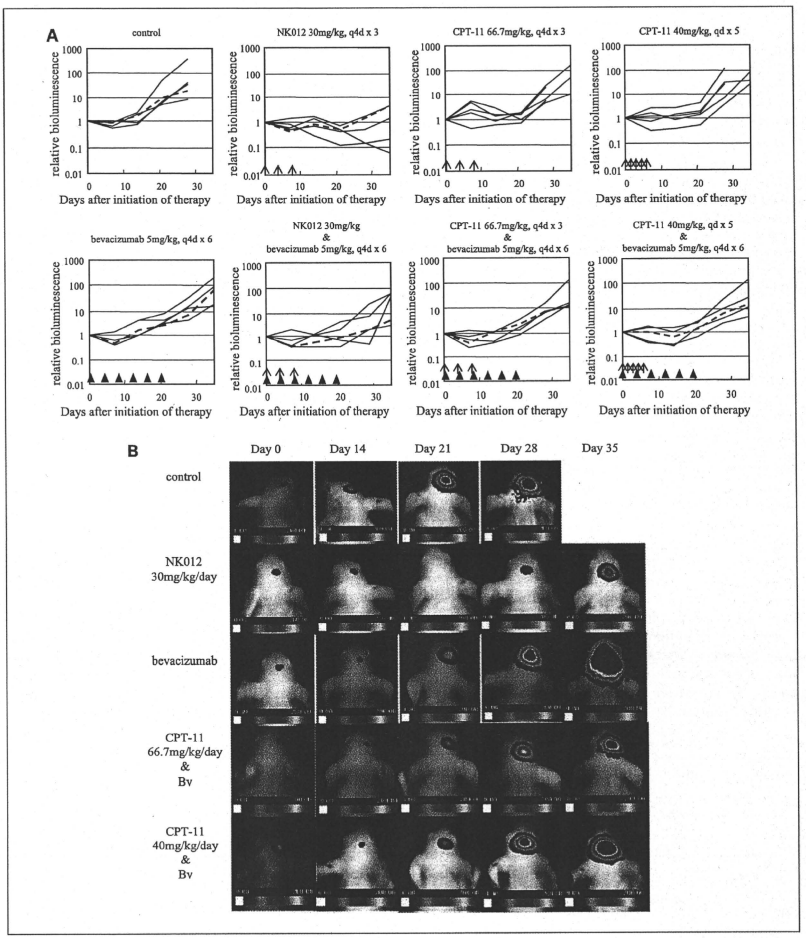

Fig. 1. Effects of NK012 and CPT-11 in U87MG/Luc mouse models. Cells were injected intracranially in athymic mice. Treatments were initiated 8 d after tumor inoculation with NK012, 30 mg/kg intravenously, thrice every 4 d; CPT-11, 67 mg/kg intravenously, thrice every 4 d; CPT-11, 40 mg/kg intravenously, daily over 5 consecutive d; bevacizumab, 5 mg/kg intraperitoneally, six times every 4 d; or both modalities and 0.9% NaCl solution control. ↑, NK012 or CPT-11 intravenous administration; ▲, bevacizumab intraperitoneal administration. *A*, antitumor activity of NK012 or CPT-11 was evaluated by counting the number of photons using the Photon Imager system. The discontinued lines in some of the graphs represent individuals that died during the experimental course and the subsequent assay was not conducted. The dashed lines correspond to the mice of each therapy expressed in *B*. *B*, images of U87MG/Luc mouse model treated with each regimen taken using the Photon Imager system on days 0, 14, 21, 28, and 35 after the initiation of therapy. Data derived from the same mice are expressed as dashed lines in *A*.

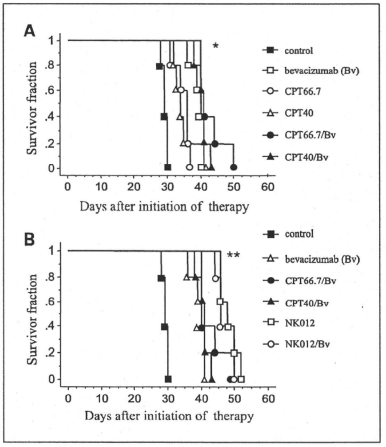

Fig. 2. Survival curves of U87MG/Luc mouse models in each regimen. *A*, ■, 0.9% NaCl solution; □, bevacizumab, 5 mg/kg, q4d × 6; ●, CPT-11, 66.7 mg/kg, q4d × 3 with bevacizumab, 5 mg/kg, q4d × 6; ▲, CPT-11, 40 mg/kg, qd × 5 with bevacizumab, 5 mg/kg, q4d × 6; ○, CPT-11, 66.7 mg/kg, q4d × 3; △, CPT-11, 40 mg/kg, qd × 5. CPT-11/bevacizumab is significantly superior to CPT-11 monotherapy [CPT66.7 versus CPT66.7/bevacizumab ($P < 0.01$) and CPT40 versus CPT40/bevacizumab ($P < 0.05$)]. *B*, □, NK012, 30 mg/kg/d, q4d × 3; ○, NK012, 30 mg/kg/d with bevacizumab, 5 mg/kg, q4d × 6; △, bevacizumab, 5 mg/kg, q4d × 6; ■, 0.9% NaCl solution; ●, CPT-11, 66.7 mg/kg, q4d × 3 with bevacizumab, 5 mg/kg, q4d × 6; ▲, CPT-11, 40 mg/kg, qd × 5 with bevacizumab, 5 mg/kg, q4d × 6. NK012 monotherapy is significantly superior to CPT66.7/bevacizumab ($P < 0.01$) and CPT40/bevacizumab ($P < 0.05$).

from the ileocecal junction for the ileum. Samples were fixed in 10 formalin, embedded in paraffin, sectioned, and stained with H&E. Inflammation was scored by using an inflammation scale from - to ++, with - indicating absent inflammation, + indicating mild inflammation predominantly infiltrated with lymphocytes, and ++ indicating active inflammation infiltrated with lymphocytes and neutrophils. All histopathologic and immunohistologic analysis and interpretation were done directly by an experienced pathologist.

Pharmacokinetics study of NK012 and CPT-11 combined with bevacizumab. Four mice bearing U87MG/Luc tumor per group were used for the biodistribution analysis of NK012 and CPT-11. Twenty-eight days after the intracranial injection of U87MG/Luc cells, NK012 (30 mg/kg) or CPT-11 (66.7 mg/kg) was intravenously administered with or without simultaneous intraperitoneal administration of bevacizumab (5 mg/kg) to the mice. After euthanasia, tumor tissues were obtained at T_{max} of each drug, 12 h after NK012 and 3 h after CPT-11 administration, respectively (12, 13). Each tumor was excised without the adjacent normal brain tissue. The size of tumor was ~5 mm in diameter. The tumor samples were rinsed with 0.9% NaCl solution, mixed with 0.1 mol/L glycine-HCl buffer (pH 3.0)/methanol at 5% (w/w), and then homogenized using Precellys 24 (Bertin Technologies). The samples were vortexed vigorously for 10 s and then filtered through an Ultrafree-MC centrifugal filter device with a cutoff molecular diameter of 0.45 μm (Millipore). We had confirmed that the filtered solution contained only free SN-38. Reverse-phase high-performance liquid chromatography was done at 35°C on a Mightysil RP-18 GP column 150 × 4.6 mm (Kanto Chemical). Fifty microliters of a sample were injected into an Alliance 2795 high-performance liquid chromatography system (Waters Associates) equipped with a Waters 2475 multi λ fluorescence detector. The mobile phase was a mixture of 100 nmol/L ammonium acetate (pH 4.2) and methanol (11:9, v/v). The flow rate was 1.0 mL/min. The content of SN-38 was calculated by measuring the relevant peak area for calibration against the corresponding peak area derived from the CPT internal standard. Peak data were recorded using a chromatography management system (MassLynx version 4.0; Waters Associates).

Statistical analysis. Data were expressed as mean ± SD. Significance of differences was calculated using the unpaired two-tailed *t* test with StatView 5.0. $P < 0.05$ was regarded as statistically significant. Kaplan-Meier analysis was done to determine the antitumor activity of each treatment on the time to morbidity, and statistical differences were ranked accordingto the Breslow-Gehan-Wilcoxon test using StatView 5.0. To evaluate the change in photon count of each treatment group, repeated-measures ANOVA was done.

Results

Antitumor response of U87MG xenograft. NK012 at the MTD (30 mg/kg/d) administered thrice every 4 days proved to be the most active against xenografts, with three tumor regressions and tumor growth delay of >18 days (Table 1). In combination with bevacizumab, CPT-11 at the MTD (66.7 mg/kg/d) administered thrice every 4 days and at the MTD (40 mg/kg/d) administered daily over 5 consecutive days induced two tumor regressions and tumor growth delay of 7 and 8 days, respectively. Without bevacizumab, CPT-11 at the MTD (40 mg/kg) administered daily over 5 consecutive days induced one tumor regression (Table 1). Comparison of the relative photon counts on repeated-measures ANOVA (days 0-28) revealed significant differences in photon counts between mice treated with NK012 and those treated with CPT-11 (66.7 mg/kg/d, q4d × 3) in combination with bevacizumab ($P = 0.02$; Fig. 1A and B). Tendency of differences between mice treated with NK012 and those treated with CPT-11 (40 mg/kg/d, qd × 5) in combination with bevacizumab ($P = 0.14$) was observed (Fig. 1A and B).

The median overall survival time was most prolonged in the NK012 (30 mg/kg/d, q4d × 3) group for 1 week

compared with the CPT-11/bevacizumab group (Table 1). The CPT-11 group with bevacizumab showed longer median overall survival time compared with the CPT-11 monotherapy group with two schedules: 66.7 mg/kg/d, q4d × 3, and 40 mg/kg/d, qd × 5, respectively (Table 1). Kaplan-Meier analysis showed a significant survival benefit of the CPT-11/bevacizumab group compared with the CPT-11 monotherapy (66.7 mg/kg/d, q4d × 3; P = 0.004) and CPT-11 (40 mg/kg/d, qd × 5; P = 0.036), respectively (Fig. 2A). Furthermore, Kaplan-Meier analysis showed a significant survival benefit in the NK012 group compared with the CPT-11 (66.7 mg/kg/d, q4d × 3)/bevacizumab group (P = 0.046) and CPT-11 (40 mg/kg/d, qd × 5)/bevacizumab group (P = 0.0041), respectively (Fig. 2B). However, there was no significant difference between NK012/bevacizumab group and NK012 monotherapy group (P = 0.45; Fig. 2B). There was no severe body weight loss or toxic death according to treatment (Table 1).

Histologic results. Histologic examinations revealed that decreased cellularity, increased tumor stroma, and inflammatory cell infiltration were observed in the tumors treated with NK012. Tumors treated with other regimens showed no apparent morphologic differences from the control tumors (Fig. 3A). Concordant with morphologic changes, the number of Ki-67$^+$ tumor cells decreased in tumors treated with NK012 compared with CPT-11/bevacizumab (Fig. 3A and B; $P < 0.001$). Quantification of VEGF-positive area and microvessel density decreased in tumors treated with NK012 compared with other treatment regimens (Fig. 3A, C, and D; $P < 0.05$). Microvessel density dramatically decreased in tumors treated with bevacizumab in combination with any formulation of the anticancer drug (Fig. 3A and C). The small intestinal mucosa of mice treated

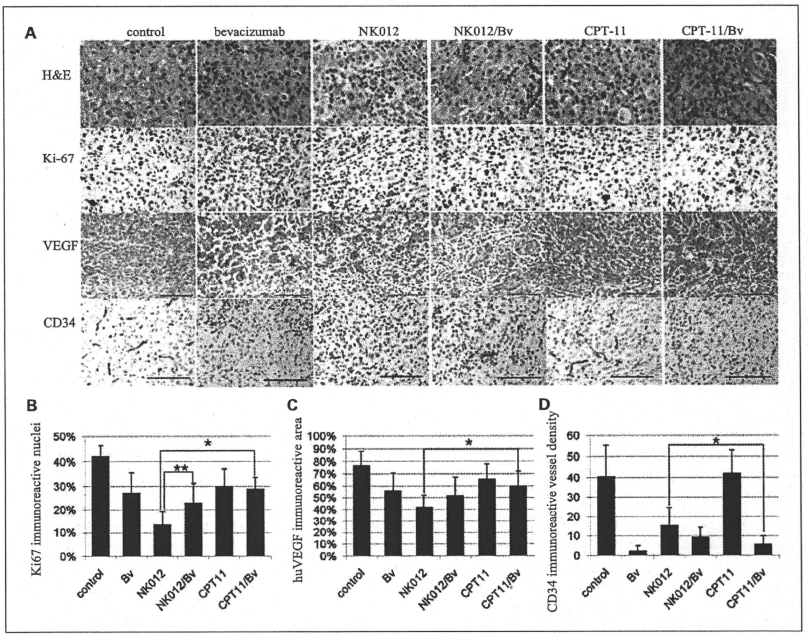

Fig. 3. Tissue-based studies of U87MG/Luc orthotopic xenografts of nude mice treated with NK012, CPT-11, bevacizumab, NK012/bevacizumab, or CPT-11/bevacizumab. *A*, H&E staining of representative xenograft regions (magnification, ×400). Immunohistochemical analysis of tumor cells stained with anti–Ki-67 nuclear antigen, anti-VEGF, and angiogenesis with anti-CD34 antibody (bar, 100 μm). Comparison between xenografts treated with each regimen. *B*, proliferation index by Ki-67. *C*, human VEGF immunoreactive area (%). *D*, angiogenesis by vessel density. *, $P < 0.01$; **, $P < 0.05$ (two-tailed Student's t test).

with NK012 or NK012/bevacizumab showed no histologic changes including fibrosis, active inflammation, or shortening and decrease in number of villi in the small intestinal mucosa as reported previously (ref. 17; data not shown).

Tissue concentration of free SN-38 after administration of NK012 and CPT-11 in combination with bevacizumab. The concentration of free SN-38 in orthotopic glioblastoma tissue after the administration of NK012 and CPT-11 in combination with bevacizumab was examined to evaluate the interaction between these anticancer agents. In the case of NK012 administration in combination with bevacizumab, free SN-38 concentration in tumor tissue was significantly decreased compared with SN-38 concentration when NK012 was administered alone (Fig. 4A; P = 0.027). On the other hand, in the case of CPT-11 administration in combination with bevacizumab, free SN-38 concentration in tumor tissue was almost similar to SN-38 concentration when CPT-11 was administered alone (Fig. 4B; P = 0.66).

Discussion

Concomitant chemoradiotherapy with surgery followed by single-agent adjuvant treatment with the alkylating agent temozolomide is the current standard of care for the patients with glioblastoma multiforme (3). However, tumor recurrence is experienced by almost all glioblastoma multiforme patients after the first-line therapy. Combination therapy of CPT-11 with bevacizumab is now a recognized second-line therapy in recurrent glioblastoma multiforme.

The main purpose of this study was to clarify the advantage of combination therapy of NK012, a SN-38–incorporating polymeric micelle, with bevacizumab against orthotopic U87MG glioblastoma multiforme tumor in mice. Single use of NK012 exerted superior antitumor activity in the orthotopic tumors compared with CPT-11 combined with bevacizumab. The NK012 single-agent treatment group showed the most prolonged survival of all treatment groups, and a statistically significant difference was revealed by the Kaplan-Meier analysis compared with the CPT-11/bevacizumab group (66.7 mg/kg/d, q4d × 3; P = 0.046 and 40 mg/kg/d, qd × 5; P = 0.0041).

The present study showed that the addition of the anti-VEGF monoclonal antibody bevacizumab to the CPT-11 therapy resulted in markedly increased activity, the same as reported clinically (9, 10). Although the mechanisms underlying the activities of bevacizumab remain unclear, the following factors are considered to be important: direct antiangiogenic effects and cytotoxics against vascular endothelial cells and other stromal elements, direct effects on tumor cells expressing VEGF receptors and stem cell–like glioma cells (18), and improvement of the delivery of anticancer drug by forced normalization of tumor vasculature (19). Bevacizumab is a humanized monoclonal antibody that does not cross-react with mouse VEGF, and the efficacy and toxicity in combination with cytotoxic drugs are not the same in mouse and human. In mice, however, bevacizumab can react with VEGF secreted from human tumor xenograft and leads to tumor vessel decrease, reduction in vessel permeability and diameter (20), and decrease in interstitial fluid pressure in xenografts (21).

NK012, a novel SN-38–incorporating polymeric micelle, is a prodrug of SN-38 similar to CPT-11. Although CPT-11 is converted to SN-38 in tumors by carboxylesterase, the metabolic conversion rate is within 2% to 8% of the original volume of CPT-11 (22, 23). In contrast, the release rate of SN-38 from NK012 is 74% under physiologic pH conditions even without carboxylesterases (12). Recently, we showed that NK012 exerted significantly more potent antitumor activity against various human tumor xenografts compared with CPT-11 (12, 24–26). The diameter of a micelle carrier is in the approximate range of 10 to 100 nm. Although this size is small, it is still sufficiently large to prevent renal secretion of the carrier. The micelle system can evade nonspecific capture by the

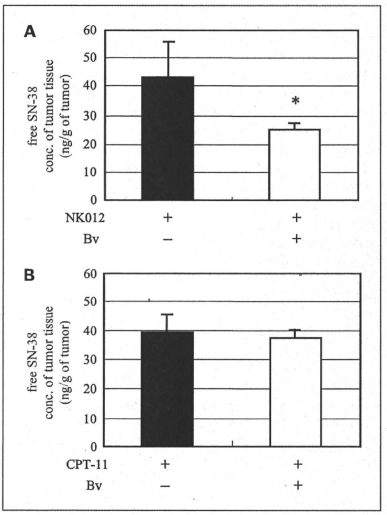

Fig. 4. Concentration of free SN-38 of tumor tissue at T_{max}. NK012 (30 mg/kg intravenously), CPT-11 (66.7 mg/kg intravenously), or bevacizumab (5 mg/kg intraperitoneally) was administered 28 d after intracranial injection of U87MG/Luc (*columns*, mean; *bars*, SD). *A*, concentration (*conc.*) of free SN-38 in glioma tissue of U87MG/Luc mouse model after administration of NK012 alone (*black column*) and NK012 with bevacizumab (*white column*). *B*, concentration of free SN-38 in glioma tissue of U87MG/Luc mouse model after administration of CPT-11 alone (*black column*) and CPT-11 with bevacizumab (*white column*). *, $P < 0.05$, significant to NK012 alone (two-tailed Student's t test).

reticuloendothelial system in various organs because the outer shell of the micelle is covered with polyethylene glycol. Therefore, a drug-incorporating micelle can be expected to have a long plasma half-life, which permits a large amount of the micelles to reach tumor tissues, extravasate from tumor capillaries, and then be retained in tumor tissues for a long time by using the enhanced permeability and retention effect (11). This prolonged retention of NK012 in the tumor and sustained release of free SN-38 from NK012 may be responsible for its more potent antitumor activity observed in the present study (27).

In this study, the antitumor effect was observed by means of bioluminescence imaging. Bioluminescence imaging revealed antitumor activity compared with CPT-11 in combination with bevacizumab. However, antiangiogenic agents can suppress the extravasation of contrast agents such as gadolinium, and gadolinium-contrast magnetic resonance imaging may give a false response (28). This means that bevacizumab is suspected of having a negative effect on bioluminescence imaging by reducing the permeability of tumor vessels. Therefore, we also evaluated the antitumor activity pathologically and immunohistochemically. Consequently, the NK012 group showed a high therapeutic advantage in Ki-67 index in a pathology analysis compared with the other treatment groups.

Interestingly, bevacizumab could not potentiate the antitumor activity of NK012 and elongate the survival of NK012. In the present pharmacologic study, the free SN-38 concentration in the tumor tissue decreased significantly when NK012 was administered in combination with bevacizumab compared with NK012 monotherapy. Results available to date and the results from the present study lead to the consideration that the reduced accumulation of NK012 by bevacizumab may cancel the direct effect of bevacizumab and NK012 against orthotopic glioma in mice. The influence of bevacizumab might be different in macromolecule such as NK012 and small compound such as CPT-11. Enhanced vascular permeability might be more important for macromolecule than small molecule. A further study is necessary to clarify the phenomenon. Dose-limiting toxicities of CPT-11 are neutropenia and diarrhea. Diarrhea was not observed in the NK012 treatment group, and the intestinal toxicity was not observed by the pathology examination as reported previously (17). As for this, it is understood that serious diarrhea has not been reported in MTD of NK012 in two phase I clinical trials against advanced solid tumors in Japan and the United States (29, 30).

In conclusion, NK012 showed a higher therapeutic index in U87MG glioblastoma in mice compared with CPT-11/bevacizumab. Therefore, data from the present study may warrant further preclinical evaluation of NK012 before conducting the clinical trial of the drug.

Disclosure of Potential Conflicts of Interest

No potential conflicts of interest were disclosed.

Acknowledgments

We thank N. Mie and M. Ohtsu for technical assistance and K. Shiina for secretarial assistance.

Grant Support

Grant-in-Aid for Third-Term Comprehensive Control Research for Cancer from the Ministry of Health, Labor and Welfare of Japan; grant 17016087 for Scientific Research on Priority Areas from the Ministry of Education, Culture, Sports, Science and Technology; and Japanese Foundation for Multidisciplinary Treatment of Cancer (Y. Matsumura) and Princess Takamatsu Cancer Research Fund 07-23908.

The costs of publication of this article were defrayed in part by the payment of page charges. This article must therefore be hereby marked *advertisement* in accordance with 18 U.S.C. Section 1734 solely to indicate this fact.

Received 9/2/09; revised 11/2/09; accepted 11/9/09; published OnlineFirst 1/12/10.

References

1. Takano S, Yoshii Y, Kondo S, et al. Concentration of vascular endothelial growth factor in the serum and tumor tissue of brain tumor patients. Cancer Res 1996;56:2185–90.
2. Kleihues P, Louis DN, Scheithauer BW, et al. The WHO classification of tumors of the nervous system. J Neuropathol Exp Neurol 2002;61:215–25, discussion 226–9.
3. Stupp R, Mason WP, van den Bent MJ, et al. Radiotherapy plus concomitant and adjuvant temozolomide for glioblastoma. N Engl J Med 2005;352:987–96.
4. Wong ET, Hess KR, Gleason MJ, et al. Outcomes and prognostic factors in recurrent glioma patients enrolled onto phase II clinical trials. J Clin Oncol 1999;17:2572–8.
5. Friedman HS, Petros WP, Friedman AH, et al. Irinotecan therapy in adults with recurrent or progressive malignant glioma. J Clin Oncol 1999;17:1516–25.
6. Cloughesy TF, Filka E, Kuhn J, et al. Two studies evaluating irinotecan treatment for recurrent malignant glioma using an every-3-week regimen. Cancer 2003;97:2381–6.
7. Chamberlain MC. Salvage chemotherapy with CPT-11 for recurrent glioblastoma multiforme. J Neurooncol 2002;56:183–8.
8. Prados MD, Lamborn K, Yung WK, et al. A phase 2 trial of irinotecan (CPT-11) in patients with recurrent malignant glioma: a North American Brain Tumor Consortium study. Neuro Oncol 2006;8:189–93.
9. Vredenburgh JJ, Desjardins A, Herndon JE 2nd, et al. Phase II trial of bevacizumab and irinotecan in recurrent malignant glioma. Clin Cancer Res 2007;13:1253–9.
10. Vredenburgh JJ, Desjardins A, Herndon JE 2nd, et al. Bevacizumab plus irinotecan in recurrent glioblastoma multiforme. J Clin Oncol 2007;25:4722–9.
11. Matsumura Y, Maeda H. A new concept for macromolecular therapeutics in cancer chemotherapy: mechanism of tumoritropic accumulation of proteins and the antitumor agent smancs. Cancer Res 1986;46:6387–92.
12. Koizumi F, Kitagawa M, Negishi T, et al. Novel SN-38-incorporating polymeric micelles, NK012, eradicate vascular endothelial growth factor-secreting bulky tumors. Cancer Res 2006;66:10048–56.